IEEE Access
Multidisciplinary | Rapid Review | Open Access Journal

Received September 9, 2019, accepted October 2, 2019, date of publication October 7, 2019, date of current version October 17, 2019.

Digital Object Identifier 10.1109/ACCESS.2019.2945868

Functional Fluid-Manipulation Using Spiral-Type Magnetic Micromachines as Micropumps, Active Valves, and Channel Selectors

DONG MIN JI AND SUNG HOON KIM, (Member, IEEE)
Department of Electronics Convergence Engineering, Wonkwang University, Iksan 54538, South Korea

Corresponding author: Sung Hoon Kim (kshoon@wku.ac.kr)

This work was supported in part by the Basic Science Research Program through the National Research Foundation of Korea (NRF), in part by the Ministry of Education, and in part by the Ministry of Science, ICT and Future Planning, under Grant NRF-2015R1D1A1A01057463 and Grant 2018R1C1B6003491.

ABSTRACT A micro-fluid manipulation technique is introduced using spiral-type magnetic micromachines as pumps, channel selector, and active valves. Magnetic micromachines, also known as microrobots, have been widely studied for biomedical applications because they offer wireless control and microscopic size. Spiral-type magnetic micromachines, which contain a screw mechanism, are synchronized by an external rotating magnetic field (the rotation of an external driving magnet). The screw mechanism means that the machines generate both propulsive and drag forces in a fluid environment. When four micromachines are installed in multi-channels they can be used to control direction and speed of rotation independently. Therefore, by controlling the direction and speed of each machine, it is possible to control the direction of fluid flow and to accelerate/decelerate the flow rate, functioning as an active valve or multiple pumps. The suitability of spiral-type magnetic micromachines for fluid manipulation in microfluid system is verified through various experiments.

INDEX TERMS Spiral-type magnetic micromachine, functional fluid manipulation, micropump, active valve, channel selecting, wireless control, synchronized magnetic radial coupling.

I. INTRODUCTION

Magnetic microrobots and their associated manipulation systems have been developed for a range of biomedical applications [1]–[5]. These robots have numerous properties that are advantageous for such applications, including wireless operation, battery-free robot bodies, microscopic size, rapid response times, and precision control. Most microrobots move within the human body and perform tasks such as precise target identification, diagnosis, drug delivery, and sensing [6]–[10]. The robots are controlled wirelessly by magnets which induce a torque or force. Magnetic forces can produce translational motion within a gradient magnetic field, whereas magnetic torque produces rotation without translational motion within a uniform magnetic field. Both types of magnetic field can be generated by permanent or electromagnets [11]–[12]. Translational movement is determined by the relationship between the robot and the magnetic field. However, rotational and alternating motions caused by magnetic torque can generate additional mechanical propulsion in the environment [13]–[16]. Mechanisms that are widely used in microrobots include screw, helical, and helical mechanisms. A uniform rotating magnetic field or rotating permanent magnet is required to rotate a robot. When a coil is used to generate a rotating magnetic field, the robot rotates in the same direction as the magnetic field. In contrast, when a permanent magnet is used, the robot rotates in the opposite direction like a magnetic gear [17]. These mechanisms generate thrust when the robot rotates in a fluid. Then, drag is generated in the opposite direction to the thrust. This is driving method used for active robotic locomotion in the fluid [18]–[20]. Drag occurs in the same direction as the fluid flow. In order words, such a robot and control method can be applied as a microfluidic control system.

Recently, many studies have investigated micropumps and valves for microfluidic control [21]–[24]. In particular, magnetically driven micropumps have been explored due to their simple control and structure. For example, Honda et al.

The associate editor coordinating the review of this manuscript and approving it for publication was Hui Xie.

developed a cylindrical micropump using an alternating magnetic field. This method used the alternating motion of an actuator composed of a NdFeB permanent magnet and an elastic film. The alternating motion of the actuator caused oscillation with moderate bending and produced unidirectional flow [28]. Shen et al. reported on a magnetic micropump that used membranes each containing an integrated permanent magnet. This was actuated by an assembled permanent magnet mounted on the rotation axis of a DC motor [29]. Pan et al. described two driving methods using planar micro-coil and micro-motor drives. In the micro-motor method, a small DC motor with permanent magnet embedded in its shaft was used to actuate a membrane mounted magnet [30]. Such magnetically actuated micropumps, have several advantages including a simple structure/configuration, wireless control (remote control), battery-free bodies, and micro size; however, they only have the pumping function.

In this study, we propose a new microfluidic control system using a spiral-type magnetic micro machine. The spiral-type machine can perform various functions in a microfluidic system including pumping, active valves, channel selection, and improved hydrodynamic performance according to the configuration of the fluid channels and machines. The fabricated machine consists of a cylindrical NdFeB permanent magnet ($\phi 1.2 \times 7.5$) and spiral blade (pitch 1.14 mm and blade angle 70°). The magnetization is in a radial direction. The machine is rotated and synchronized by the rotation of external magnet (see Fig. 1). Typically, spiral mechanisms are applied to axial pumps in fluid channels or pipes. However, when the spiral machine rotates, it produces rotating fluid flow in addition to axial flow. In addition, we controlled the direction of drag and rotation speed of the machines so that they would function as active valves and prevent fluid flow. When the various drag forces occur in the same direction the pressure in the channel increases. This is equivalent to a series connection used to increase the pressure in a multipump configuration. In general, independent pumps, valves, etc. are used in fluid control systems; this results in complex structures. We propose and experimentally verify the viability of replacing pump, valve, and channel selection functions with a spiral-type magnetic machine in multi-channels.

II. METHODS FOR WIELESS CONTROL AND FLUID MANIPULATION

A. MAGNETIC WIRELESS CONTROL

For fluid manipulation, we utilized a spiral-type magnetic micromachine and a wireless magnetic control method. Two driving methods can be used to rotate the machine: a uniform rotating magnetic field with an electromagnetic control (EM control) or magnetic coupling using a permanent magnet (PM control). If the machine does not need to be mobile, PM control is better than EM control. Figure 1 (a) illustrates the synchronous magnetic radial coupling mechanism between two magnets used for PM control. The rotational mechanism of this configuration can be considered a magnetic gear.

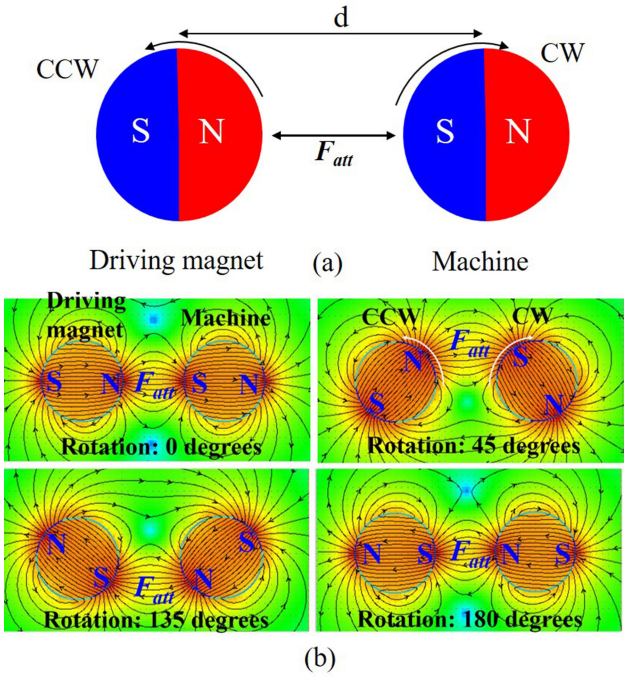

FIGURE 1. Method used for magnetic wireless control. (a) Synchronous magnetic radial coupling between the driving magnet and the machine, where F_{att} is the magnetic radial coupling force (attractive force). (b) Combined magnetic flux in the radial coupling according to the angle of rotation. CCW and CW indicate the counterclockwise and clockwise direction, respectively.

When the driving magnet rotates counterclockwise (CCW), the machine rotates clockwise (CW) because of the magnetic coupling force.

Before the driving magnet and the machine being to rotate, an attractive magnetic force is generated as a result of their alignment. As the driving magnet rotates, the machine rotates in the opposite direction to preserve this coupling, as shown in Fig. 1(b). Figure 1 (b) shows the magnetic radial coupling between two permanent magnets for different angles of rotation. This shows the variations in the combined coupling field flux (position of maximum magnetic radial coupling force $\boldsymbol{F}_{att}$). In this driving method, the coupling force (attractive force) is very important. It determines the rotation of the machine.

As the coupling force increases, the starting torque increases, and the driving range of the maximum rotation speed becomes wider. The magnetic coupling force can be expressed as [31]:

$$\begin{aligned} \boldsymbol{F} &= \sum_{V} \nabla[\boldsymbol{m}\mu_0(\boldsymbol{x},\boldsymbol{y},\boldsymbol{z}) \cdot \boldsymbol{H}_{ext} \\ &= \int_{V} \nabla[\boldsymbol{M}\mu_0(\boldsymbol{x},\boldsymbol{y},\boldsymbol{z}) \cdot \boldsymbol{H}_{ext}]\boldsymbol{dV} \end{aligned} \tag{1}$$

where μ_0 is the permeability of free space, V is the volume of the magnetic machine, $\boldsymbol{M}$ is the magnetization of the machine, $\boldsymbol{H}_{\mathbf{ext}}$ is the external magnetic field strength, and $\boldsymbol{m} = \boldsymbol{MdV}$.

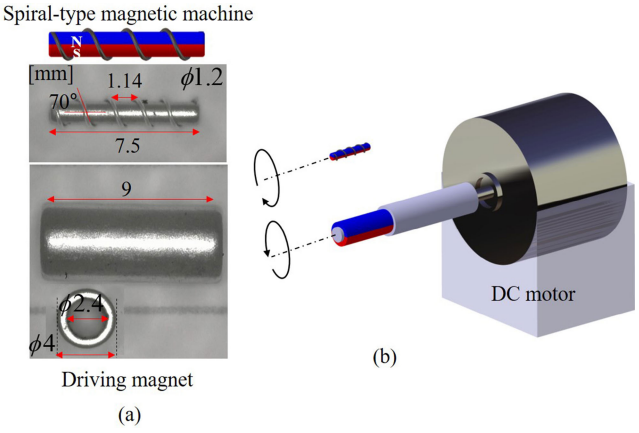

FIGURE 2. (a) Fabricated spiral-type magnetic micromachine and driving magnet. (b) Configuration for magnetic radial coupling between the machine and the driving magnet.

If we consider the position between the machine and the driving magnet on the x-axis, the magnetic coupling force can be expressed as:

$$\begin{aligned} \boldsymbol{dF} &= \nabla(\mu_0 \boldsymbol{m} \cdot \boldsymbol{H_{ext}}) = \mu_0 \boldsymbol{M} \mathrm{dS} dx \frac{\partial \boldsymbol{H_{ext\_x}}}{\partial x} \\ \boldsymbol{F_x} &= \mu_0 \boldsymbol{M} \int \mathrm{dS} \frac{\partial \boldsymbol{H_{ext\_x}}}{\partial x} \boldsymbol{dx} \end{aligned} \tag{2}$$

where $\boldsymbol{dF}$ is the infinitesimal coupling force between the driving magnet and the machine, $\boldsymbol{H_{ext\_x}}$ is the magnetic field strength in the x direction, d is the thickness of the driving magnet, and S is the polar surface. The magnetic coupling force is controlled by the distance between the driving magnet and the machine. Figure 2 (a) shows the fabricated magnetic machine with the driving magnet (cylindrical NdFeB $\phi 4 \times \phi 2.4 \times 9$mm). The machine, which consists of a cylindrical NdFeB bar magnet of $\phi 1.2 \times 7.5$mm and spiral blade with pitch of 1.14 mm and blade angle of 70°, is synchronized with the rotation of the driving magnet because the two magnets have diametric magnetization. The driving magnet is connected to a DC motor and the rotation speed is controlled by pulse width modulation (PWM). In order to observe the driving conditions, we changed the coupling distance, whereas all of the fluid control experiments were performed at a fixed coupling distance of approximately 8 mm. Figure 2 (b) shows basic concept of synchronized magnetic radial coupling between the driving magnet and the machine.

B. METHOD FOR FLUID MANIPULATION

Figure 3 shows principle of fluid manipulation according to changes in the direction and speed of rotation of the machine when it is used as a pump, valve, or channel selector. When the machine has a right-hand screw mechanism, CW rotation produces fluid flow in the CW direction (Flow_1) and axial fluid flow in the backward direction (Flow_2), as shown in Fig. 3 (a1). In contrast, CCW rotation produces fluid flow in the CCW direction (Flow_1) and axial flow in the forward direction (Flow_2), as shown in Fig. 3 (a2). Flow_1 is caused by centrifugal force from the rotation of the machine, whereas Flow_2 is caused by the spiral blade on the machine.

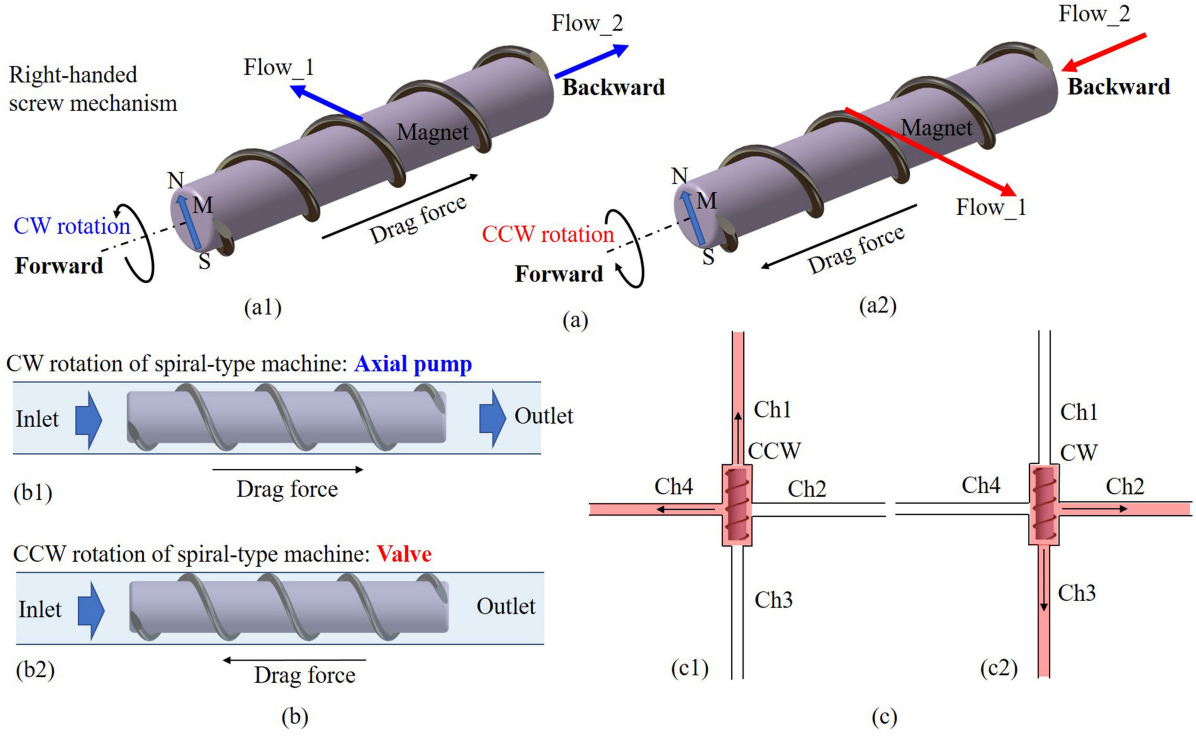

FIGURE 3. (a1 and a2) Direction of fluid flow when the machine rotates CW or CCW, respectively. (b1 and b2) Micropump and valve concepts in the microchannel, respectively. (c) Fluid channel selection achieved by controlling the rotation direction of the machine.

Figure 3 (b) shows the case where the machine is used as an axial-flow pump with a valve in one channel. If the machine has a right-handed screw mechanism, CW rotation produces a pumping action in the fluid channel. This is an axial-flow pump, as shown in Fig 3 (b1). In contrast, with CCW fluid flow is restricted by the direction of drag because of the spiral structure (right-handed screw), as shown in Fig. 3 (b2). The machine then becomes an active valve due to the rotation speed of the machine. By controlling the rotation speed of the machine the hydrodynamic performance can be controlled.

As described above, the rotation of the machine provides two fluid flows: Flow_1 and Flow_2. Furthermore, the direction, in which the machine rotates, determines the direction of Flow_1 and Flow_2. CCW direction selects Ch4 and Ch1, as shown in Fig. 3 (c1), and CW direction selects Ch2 and Ch3, as shown in Fig. 3 (c2). Therefore, when the machine is installed in the multi-channel, we control the direction of rotation in order to select a channel. In experimental analysis (Section III), we verified these proposed functions.

III. EXPERIMENTAL ANALYSIS AND DISCUSSION

A. DRIVNG CONDITIONS FOR SYNCHRONIZED MAGNETIC RADIAL COUPLING

The range of the synchronized rotation speed is dependent on the magnetic radial coupling force. This force is determined by the distance between the driving magnet and the machine. We observed the magnetic coupling force at intervals of 1 mm up to 16 mm using a digital force gauge (IMADA DS2-2N); the results are shown in Fig. 4 (a). The coupling force had a peak of 0.48 N at 1 mm and decreased rapidly up to 3 mm (0.13 N). Above this distance, the coupling force decreased slowly, from 0.062 N at 4 mm to 0.0005 N at 16 mm. We then assessed the change in power consumption at the starting point of the rotation of the machine as the coupling distance increased; the results are shown in Fig. 4 (b). The power consumption increased as the coupling distance decreased, this is a disadvantage of strong coupling forces. Furthermore, we recorded the maximum rotation speed of the machine using a Hall sensor at different distances; the results are shown in Fig. 4 (c). The machine rotated in fluid. The greatest range of rotation speed was obtained at small coupling distances. A coupling distance of 2 mm resulted in a coupling force of 0.17 N and power consumption of 36.3 mW. Under these conditions, the machine achieved a rotation speed of 14100 rpm. When the distance increased to 16 mm, the coupling force, power consumption, and maximum rotating speed were 0.1 mN, 24.3 mW, and 6800 rpm, respectively. Fluid control experiments with an actual machine were conducted at a coupling distance of 8 mm. This results in a coupling force, power consumption, and maximum rotational speed of 0.012 N, 26.79 mW, and 13500 rpm, respectively. Coupling distances up to 8 mm can guarantee a rotation speed of 12000 rpm. Therefore, all experiments maintain a coupling distance of 8 mm.

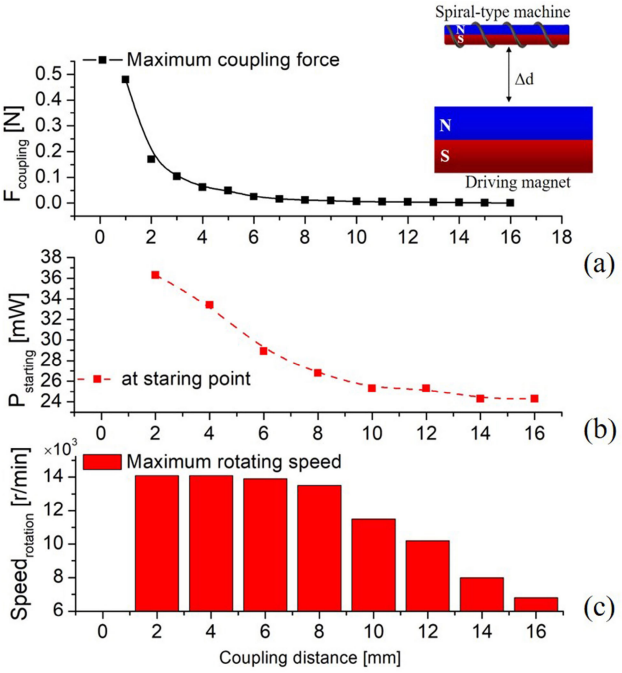

FIGURE 4. Variation in (a) radial coupling force between the machine and the magnet, (b) power consumption at the starting point of the rotation, and (c) maximum rotation speed against changes in the coupling distance.

B. PUMPING ABILITY AND CONTROL OF FLOW DIRECTION

A rotating the spiral-type magnetic micromachine can be applied to fluid manipulation in a fluid environment because of the spiral mechanism. The machine is applied to a wide range of Reynolds number ($10^{-7} < \mathrm{Re} < 10^{3}$). First, we assessed basic pumping abilities according to changes in the rotation speed of the machine up to 6000 rpm. Figure 5 (a1) compares the maximum pump heads against in the rotation speed of the machine with water and silicone oil (100 cst). The pump head is proportional to the rotation speed. The water and silicone oil have different viscosities, this means that the pump heads are different at the same rotational speed. The fabricated machine produced minimum pump heads of 50 and 550 Pa at 1800 rpm, and maximum pump heads of 430 and 1480 Pa at 6000 rpm with water and silicone oil, respectively.

The flow rates of silicone oil and water were greatest when the rotation speed of the machine was between 1800 and 6000 rpm and the pump head was zero, as shown in Fig. 5 (a2). The maximum flow rate is achieved when the pump head is zero. Under this condition, the rotation speeds of 1800, 4200, and 6000 rpm in the silicone coil produced flow rates of 0.1814, 0.3389, and 0.5539 mL/min, respectively. The machine produced flow in two directions due to the spiral mechanism and direction of rotation: axial flow (Flow_2) and centrifugal flow (Flow_1). Figure 5 (a3) shows the fluid velocity of Flow_1 and Flow_2 when the machine rotated CW at between 3000 and 11000 rpm.

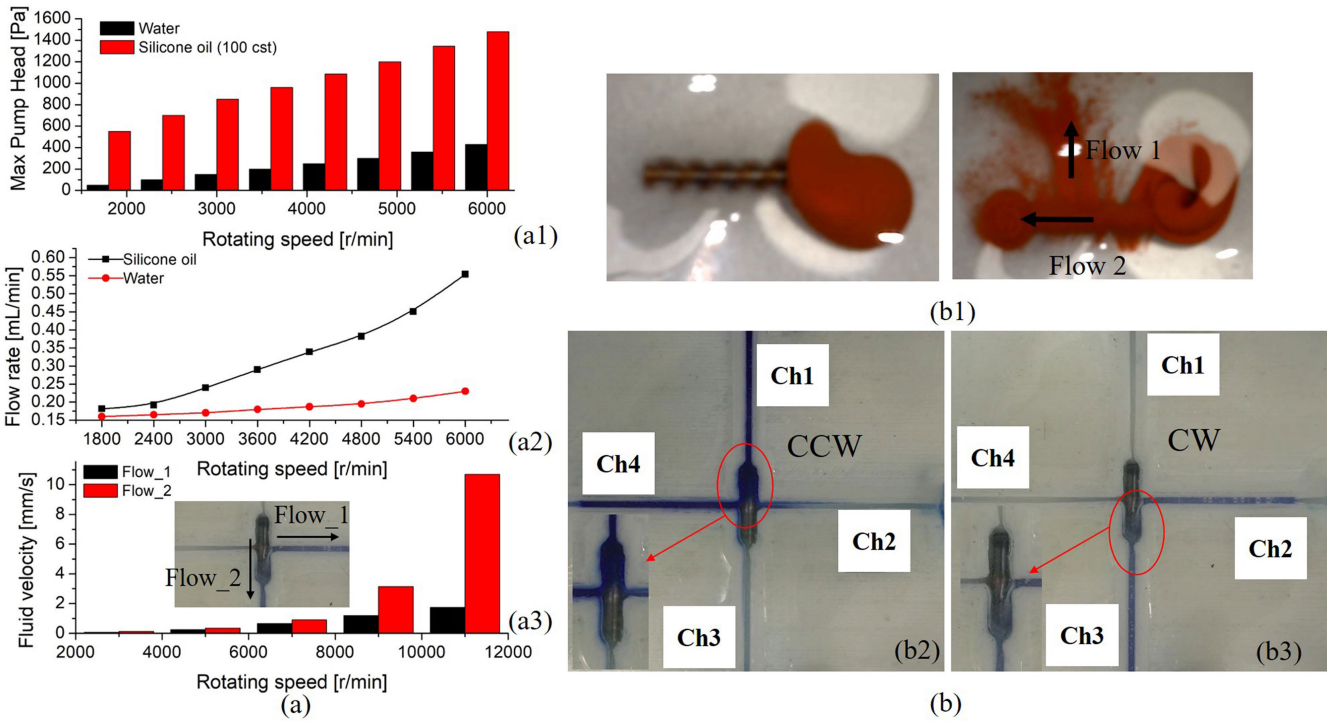

FIGURE 5. (a) Hydrodynamic performance: (a1) Maximum pump head of water and silicone oil (100 cst) according two changes in the rotating speed of the machine, (a2) variations in flow rate according to changes in the rotating speed, and (a3) Fluid velocities of axial flow (Flow_2) and later flow (Flow_1) in the fabricated microchannels. (b) Control of fluid flow (Top view): (b1) Observation of the two flows in the silicone oil without the channel. (b2 and b3) Verification of selecting the channel by the rotating direction of the machine.

To measure the fluid velocity, we fabricated fluid channels 0.7 mm wide and 2.5 mm deep using a 3D printer. As the rotation speed of the machine increased, velocity of both fluid flows changed significantly. In the fabricated channels, the minimum and maximum velocities of Flow_1 were 0.066 and 1.74 mm/S at 3000 and 11000 rpm, respectively. Flow_2 produced minimum and maximum velocities of 0.12 and 10.7 mm/s at equivalent velocities. In general, axial-flow pumps require relatively high rotation speeds compared to centrifugal pumps in order to obtain the pumping ability. Centrifugal pumps can discharge large flow rates even at relatively low rotation speeds because they have sufficient space for the fluid to be discharged by the centrifugal force of the machine. In particular, because of the spiral structure and the difference between the size of the channel (0.7 mm wide) and the machine (1.2 mm thick and 7.5 mm long), axial flow was the major flow direction.

We conducted experiments in order to confirm the effect of the rotation direction of the machine on the flow direction, as shown in Fig. 5 (b). Figure 5 (b1) represents Flow_1and Flow_2 in silicone oil (100 cst) without channels. The machine has a left-handed spiral structure so the driving magnet rotated CW which caused the machine to rotate CCW at 3000 rpm. Under this condition, two directions of flow were observed using yellow oil paint: Flow_1 and Flow_2. We experimented to select the channel in the same direction as the rotation of the machine by applying the basic mechanism to multiple channels. In this experiment, the machine had a right-handed spiral mechanism and rotated at 3000 rpm. We prepared four channels for flow direction and installed the machine on a test bed in the center. Silicone oil was injected in the same location of the machine (center of machine) via a syringe pump at a rate of 20 μL/min. We began by rotating the machine CCW. In this case, the drag on the fluid was in the Ch1 direction and the rotation of the machine was in the Ch4 direction. Therefore, the fluid moved along Ch1 and Ch4, as shown in Fig. 5 (b2). In contrast, when the machine rotated CW, the fluid moved in the direction of Ch2 and Ch3, as shown in Fig. 5 (b3). The direction of thrust and drag were opposite to each other. Hence, the spiral machine can be used select the fluid channel by controlling the direction of rotation.

C. ACTIVE VALVE AND FLIUD MIXER

Active valves are one of the possible applications for this machine. Figure 6 shows its performance as an active valve (front view). For this experiment, we used two machines with right-handed spiral. Machine 1 was designed to function as an active valve and Machine 2 was designed to function as a micropump. When the direction of drag from Machine 1 is opposite to the direction of drag from Machine 2, Machine 1 functions as an active valve. If the drag forces from Machines 1 and 2 are in the same direction, the configuration functions as a dual pump and increases the pump head. Next, we reversed the directions of the drag from Machines 1 (CCW) and 2 (CCW).

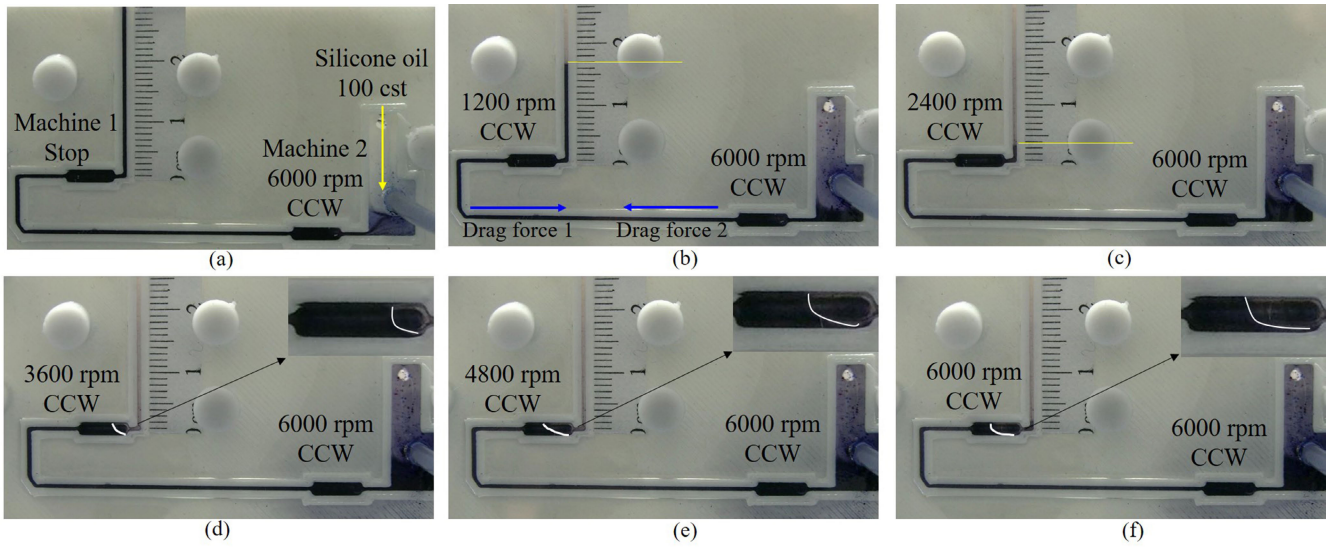

FIGURE 6. Verification of performance as an active valve (Machine 1) using the spiral machine (front view) and the change in fluid movement with increasing rotation speed. (a) Rotation stop of Machine 1 with 100% open valve. (b to f) Displacement of the fluid when Machine 1 rotated at 1200, 2400, 3600, 4800, and 6000 rpm, respectively.

The rotating speed of Machine 2 was constant at 6000 rpm and the rotating speed of Machine 1 increased up to 6000 rpm at 1200 rpm intervals while the displacement of the fluid was observed. First, Machine 1 was stationary while Machine 2 rotated CCW at 6000 rpm. At this point, fluid flowed past Machine 1 and the pump head increased. Since the drag from Machine 1 was zero, the valve was open, as shown in Fig. 6(a). Second, the rotation speed of Machine 1 increased in CCW direction which caused the displacement (pump head) of fluid to decrease. For example, when the rotation speed of Machine 1 changed from 1200 to 2400 rpm, the height of the fluid decreased from 16 to 3 mm. The silicone oil could not pass through Machine 1 when it rotated at 3600 rpm, as shown in Fig. 6 (b) to (d). In addition, at speeds of 4800 and 6000 rpm, the fluid decreased even more in the space around Machine 1, as shown in Fig. 6 (e) and (f).

Figure 7 shows the performance of the device as a mixer and as a pump. In this test, Machines 1 and 2 were used as micropumps and Machine 3 was applied as a mixer. The three machines had right-handed spiral structures and rotated CW, CCW, and CCW, respectively, at 3000 rpm. Due to the pumping ability of Machines 1 and 2, the blue and red oils are present at outputs 1 and 3. The purple oil appeared at output 2 because Machine 3 mixed the blue and red oils.

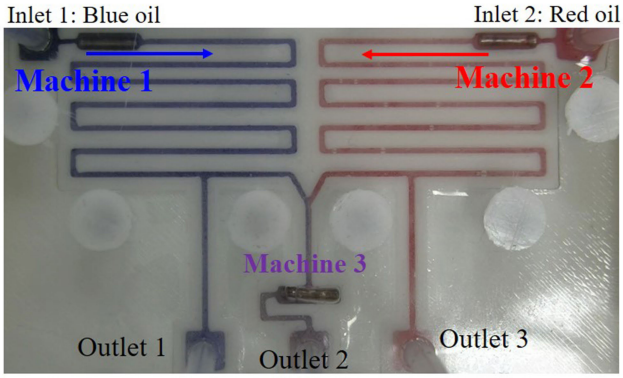

	Machine 1	Machine 2	Machine 3
Direction and speed	CW and 3000 rpm	CCW and 3000 rpm	CCW and 3000 rpm
Function	Pumping	Pumping	Mixing
Oil color	Outlet1:Blue	Outlet3: Red	Outlet2: Purple

FIGURE 7. Observation and conditions of two pumps and a mixer using three machines (top view).

D. PROGRAMMABLE AND FUNCTIONAL FLUID MANIPULATION

To verify the viability of fluid manipulation using the spiral-type magnetic micromachine, we prepared four machines and multiple channels, as shown in Fig. 8 (a). Four driving magnets were installed at the four DC motors. We configured the control system using LabVIEW software to control the speed and direction of the motor. The control system generated a PWM (Pulse Width Modulation) signal to each motor to control the rotation speed of the machine. The duty ratio of the PWM is adjusted by observing the rotational speed of the machine using a Hall sensor. In order to achieve fluid manipulation in the channels, we controlled the direction of rotation of the machines at fixed speeds of 6000 rpm. The test bed consisted of three inputs, seven outputs, and nine channels with four machines. The three inputs were yellow (Y), purple (P), and blue (B) oils (100 cst).

Figure 8 (b) shows the fluid flows and the color of the oils in the channels. Machines 1, 2, 3, and 4 initially rotated CCW, CW, CCW, and CCW, respectively. Under these conditions, Machines 1, 2, 3, and 4 selected Ch1 and Ch2, Ch4 and Ch7,

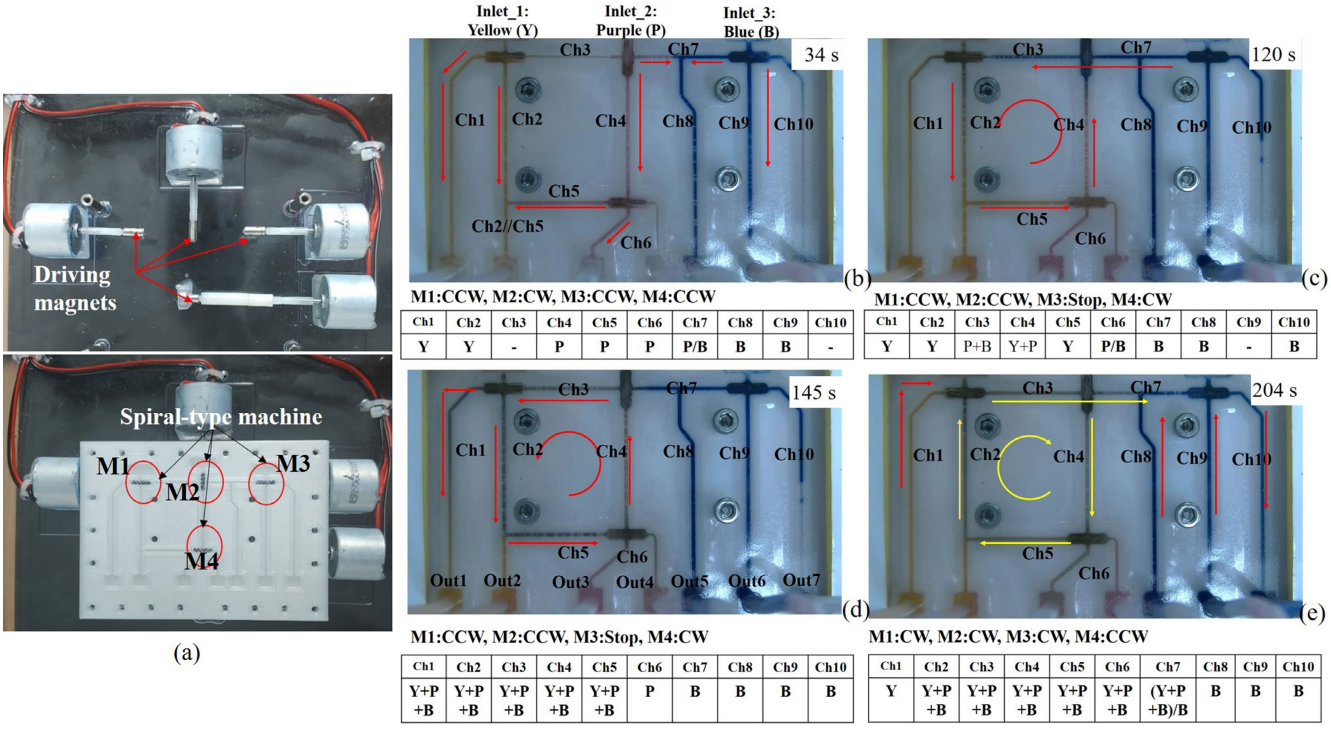

M1:CCW, M2:CW, M3:CCW, M4:CCW

Ch1	Ch2	Ch3	Ch4	Ch5	Ch6	Ch7	Ch8	Ch9	Ch10
Y	Y	-	P	P	P	P/B	B	B	-

M1:CCW, M2:CCW, M3:Stop, M4:CW

Ch1	Ch2	Ch3	Ch4	Ch5	Ch6	Ch7	Ch8	Ch9	Ch10
Y	Y	P+B	Y+P	Y	P/B	B	B	-	B

M1:CCW, M2:CCW, M3:Stop, M4:CW

Ch1	Ch2	Ch3	Ch4	Ch5	Ch6	Ch7	Ch8	Ch9	Ch10
Y+P +B	Y+P +B	Y+P +B	Y+P +B	Y+P +B	P	B	B	B	B

M1:CW, M2:CW, M3:CW, M4:CCW

Ch1	Ch2	Ch3	Ch4	Ch5	Ch6	Ch7	Ch8	Ch9	Ch10
Y	Y+P +B	Y+P +B	Y+P +B	Y+P +B	Y+P +B	(Y+P +B)/B	B	B	B

FIGURE 8. (a) Configuration of control system for functional fluid control system. (b) Initial flows of the three inputs and the rotating conditions of the four machines. (c and d) Fluid circulations (Ch3→Ch2→Ch5→Ch4→Ch3) in CCW direction and the changed colors in the channels. (e) CW circulation (Ch3→Ch4→ Ch5→Ch2) and the conditions of the machines.

Ch7 and Ch9, and Ch5 and Ch6, respectively. When operated at the same rotation speed, the velocity of the axial flow from Machine 3 was faster than the centrifugal flow velocity from Machine 2. Therefore, the oil in Ch8 was blue. In addition, the flow in Ch7 from Machine 2 prevented the movement of blue oil, so it functioned as a closed valve. Next, we performed a test in which the fluid was circulated in the order Ch3→Ch2→Ch5→Ch4 (CCW circulation) by controlling the rotation direction of the machines, as shown in Fig. 8 (c). In this case, the operating conditions of the four machines were CCW, CCW, Stationary, and CW, respectively. The colors in Ch3, Ch2, Ch5, and Ch4 were P+B, Y, Y, and Y+P, respectively. After 25 s under these conditions, the color of the fluid in the channels changed due to the circulation of the fluid, as shown in Fig. 8 (d). To change the direction of circulation from Ch3→Ch 2→ Ch5→Ch4 (CCW circulation) to (Ch3→Ch4→Ch5&Ch6→Ch2)//Ch7, the rotation directions of the four machines were changed to CW, CW, CW, and CCW, respectively, as shown in Fig. 8(e). Therefore, Machine 1 selected Ch 2 and Ch3, Machine 2 selected Ch4 and Ch7, and Machine 4 selected Ch5 and Ch6. Machine 3 rotated CW to move the fluid from Ch7 to Ch9 and Ch10. This helped to move the fluid flowing along the right side of Machine 2. If Machine 3 rotated CCW, the fluid in Ch3 was unable to move to Ch7 because Machine 3 functioned as a valve due to the direction the drag from Machine 3.

Through these experiments, we were able to verify the viability of the proposed method of functional fluid control using the spiral-type magnetic micromachine. In the fabricated fluid control environment, the direction of fluid flow was controlled using the direction and speed of rotation of the machines, and the machine performed a pump, mixer, and valve. In general, microfluid control systems require independent micropumps, mixers, and valves to operate multi-channels which results in a complex structure and configuration. Therefore, the proposed method using the spiral-type magnetic micromachines and magnetic coupling for wireless operation has great potential. In particular, the machine can be rotated bi-directionally to control the direction of fluid flow. Furthermore, the hydrodynamic properties can be controlled by connecting multiple machines. For example, if two machines are connected in parallel with the same rotation speed, the flow rate of the fluid is doubled. Alternatively, if two machines are connected in series, the pressure of the fluid doubles when the drag forces on the two fluids are in the same direction.

IV. CONCLUSION

Spiral-type magnetic micromachines are widely used in various biomedical fields. Because the machines are controlled by an external magnetic field and have mobility, they are mainly used for diagnosis and therapy in the human body. When the machine rotates in the fluid, it generates thrust and drag acts on the fluid in the opposite direction to the thrust. This can be used to control fluid flow. In general, spiral, helical, and screw mechanisms can be applied to a

propeller for axial pumping, whereas we used two flows in the axial and lateral directions through the rotation of the machine. When we controlled the direction of rotation of the machine, we were able to select the flow direction via the spiral mechanism (right or left-handed mechanism). For the experiments, we controlled the speed and direction of rotation of the four motors individually using LABVIEW software.

In this study, we verified that it was possible to achieve functional fluid control using spiral machines by controlling the speed and direction of rotation of the machines in multi-channels. In particular, we were able to verify the functionality of the pumps, valves and mixers by controlling four machines individually in multiple channels to control fluid flow direction. In addition, we verified each function experimentally using basic hydrodynamic properties and confirmed their applicability to the microfluidic control system of the machine.

REFERENCES

[1] A. Ghosh and P. Fischer, "Controlled propulsion of artificial magnetic nanostructured propellers," *Nano Lett.*, vol. 9, no. 6, pp. 2243–2245, May 2009.

[2] B. J. Nelson, I. K. Kaliakatsos, and J. J. Abbott, "Microrobots for minimally invasive medicine," *Annu. Rev. Biomed. Eng.*, vol. 12, pp. 55–85, Aug. 2010.

[3] S. H. Kim and K. Ishiyama, "Magnetic robot and manipulation for active-locomotion with targeted drug release," *IEEE/ASME Trans. Mechatronics*, vol. 19, no. 5, pp. 1651–1659, Oct. 2014.

[4] S. Tasoglu, E. Diller, S. Guven, M. Sitti, and U. Demirci, "Untethered micro-robotic coding of three-dimensional material composition," *Nature Commun.*, vol. 5, Jan. 2014, Art. no. 3124.

[5] J. Giltinan, E. Diller, and M. Sitti, "Programmable assembly of heterogeneous microparts by an untethered mobile capillary microgripper," *Lab Chip*, vol. 16, no. 22, pp. 4445–4457, Oct. 2016.

[6] S. Pane, O. Ergeneman, K. M. Sivaraman, T. Lühmann, H. Hall, and B. J. Nelson, "Strategies for drug-delivery and chemical sensing using biomédical microrobots," in *Proc. IEEE Int. Conf. Nano/Mol. Med. Eng.*, Dec. 2010, pp. 148–152.

[7] S. Yim and M. Sitti, "Shape-programmable soft capsule robots for semi-implantable drug delivery," *IEEE Trans. Robot.*, vol. 28, no. 5, pp. 183–194, Oct. 2012.

[8] A. K. Hoshiar, T.-A. Le, F. U. Amin, M. O. Kim, and J. Yoon, "Studies of aggregated nanoparticles steering during magnetic-guided drug delivery in the blood vessels," *J. Magn. Magn. Mater.*, vol. 427, pp. 181–187, Apr. 2017.

[9] H. M. Ko and S. H. Kim, "Preliminary validation of robotic control of magnetic particles for targeted hyperthermia," *J. Mang.*, vol. 23, no. 1, pp. 117–124, Mar. 2018.

[10] J. Nam, W. Lee, J. Kim, and G. Jang, "Magnetic helical robot for targeted drug-delivery in tubular environments," *IEEE/ASME Trans. Mechatronics*, vol. 22, no. 6, pp. 2461–2468, Dec. 2017.

[11] M. B. Khamesee, N. Kato, Y. Nomura, and T. Nakamura, "Design and control of a microrobotic system using magnetic levitation," *IEEE/ASME Trans. Mechatronics*, vol. 7, no. 1, pp. 1–14, Mar. 2002.

[12] K. E. Peyer, S. Tottori, F. Qui, L. Zhang, and B. J. Nelson, "Magnetic helical microcomponents," *Chem. Eur. J.*, vol. 19, no. 1, pp. 28–38, 2013.

[13] M. T. Hou, H.-M. Shen, G.-L. Jiang, C.-N. Lu, I.-J. Hsu, and J. A. Yeh, "A rolling locomotion method for untethered magnetic microrobots," *Appl. Phys. Lett.*, vol. 96, no. 2, pp. 024102-1–024102-3, Jan. 2010.

[14] S. Sudo, S. Segawa, and T. Honda, "Magnetic swimming mechanism in a viscous liquid," *J. Intell. Mater. Syst. Struct.*, vol. 17, nos. 8–9, pp. 729–736, Sep. 2006.

[15] T. Honda, K. I. Arai, and K. Ishiyama, "Micro swimming mechanisms propelled by external magnetic fields," *IEEE Trans. Magn.*, vol. 32, no. 5, pp. 5085–5087, Sep. 1996.

[16] J. J. Abbott, O. Ergeneman, M. P. Kummer, A. M. Hirt, and B. J. Nelson, "Modeling magnetic torque and force for controlled manipulation of soft-magnetic bodies," *IEEE Trans. Robot.*, vol. 23, no. 6, pp. 1247–1251, Dec. 2007.

[17] M. K. Song and S. H. Kim, "Wireless magnetic pump: Characteristics of magnetic impellers and medical application," *J. Mang.*, vol. 22, no. 2, pp. 344–351, Jun. 2017.

[18] S. H. Kim, K. S. Shin, S. Hashi, and K. Ishiyama, "A pushing force mechanism of magnetic spiral-type machine for wireless medical-robots in therapy and diagnosis," *IEEE Trans. Magn.*, vol. 49, no. 7, pp. 3488–3491, Jul. 2013.

[19] A. Barbot, D. Decanini, and G. Hwang, "Helical microrobot for force sensing inside microfluidic chip," *Sens. Actuators A, Phys.*, vol. 266, no. 15, pp. 258–272, Oct. 2017.

[20] K. E. Peyer, L. Zhang, and N. J. Nelson, "Bio-inspired magnetic swimming microrobots for biomedical applications," *Nanoscale*, vol. 5, no. 4, pp. 1259–1272, Nov. 2012.

[21] J. G. Smits, "Piezoelectric micropump with three valves working peristaltically," *Sens. Actuators A, Phys.*, vol. 21, nos. 1–3, pp. 203–206, Feb. 1990.

[22] E. Zordan, F. Amirouche, and Y. Zhou, "Principle design and actuation of a dual chamber electromagnetic micropump with coaxial cantilever valves," *Biomed. Microdevices*, vol. 12, no. 1, pp. 55–62, Feb. 2010.

[23] V. Singhal and S. V. Garimella, "Induction electrohydrodynamics micropump for high heat flux cooling," *Sens. Actuator A. Phys.*, vol. 134, no. 2, pp. 650–659, Mar. 2007.

[24] A. Hatch, A. E. Kamholz, G. Holman, P. Yager, and K. F. Bohringer, "A ferrofluidic magnetic micropump," *J. Microelectromech. Syst.*, vol. 10, no. 2, pp. 215–221, Jan. 2001.

[25] K. S. Ryu, K. Shaikh, E. Goluch, Z. Fan, and C. Liu, "Micro magnetic stir-bar mixer integrated with parylene microfluidic channels," *Lab Chip.*, vol. 4, no. 6, pp. 608–613, 2004.

[26] J. K. Hamilton, M. T. Bryan, A. D. Gilbert, F. Y. Ogrin, and T. O. Myers, "A new class of magnetically actuated pumps and valves for microfluidic applications," *Sci. Rep.*, vol. 8, no. 1, Jan. 2018, Art. no. 933.

[27] T. Sawetzki, S. Rahmouni, C. Bechinger, and D. W. Marr, "*In situ* assembly of linked geometrically coupled microdevices," *Proc. Nat. Acad. Sci. USA*, vol. 105, no. 51, pp. 20141–20145, 2008.

[28] T. Honda, A. Yoshida, and J. Yamasaki, "Cylindrical micropump driven by external magnetic fields," *Int. J. Appl. Electromagn. Mach.*, vol. 25, nos. 1–4, pp. 511–516, May 2007.

[29] M. Shen, L. Dovat, and M. A. M. Gijs, "Magnetic active-valve micropump actuated by a rotating magnetic assembly," *Sens. Actuat. B. Chem.*, vol. 154, no. 1, pp. 52–58, May 2011.

[30] T. Pan, S. J. McDonald, E. M. Kai, and B. Ziaie, "A magnetically driven PDMS micropump with ball check-valves," *J. Micromech. Microeng.*, vol. 15, no. 5, pp. 1021–1026, Mar. 2005.

[31] S. H. Kim, S. Hashi, K. Ishiyama, Y. Shiraishi, Y. Hayatus, M. Akiyama, Y. Saiki, and T. Yambe, "Preliminary validation of a new magnetic wireless blood pump," *Artif. Organs*, vol. 37, no. 10, pp. 920–926, Oct. 2013.

DONG MIN JI received the B.Sc. degree in electronics convergence engineering from Wonkwang University, Iksan, South Korea, in 2019, where he is currently pursuing the M.Eng. degree. His current research interest includes design and control of magnetic actuators and microrobots.

SUNG HOON KIM (M'12) received the B.S. degree in electronic engineering from Yeungnam University, Gyeongsan, South Korea, in 2005, the M.S. degree in medical and biological engineering from Kyungpook National University, Daegu, South Korea, in 2007, and the Ph.D. degree in electrical communication engineering from Tohoku University, Sendai, Japan, in 2012. He is currently an Associate Professor with the Department of Electronics Convergence Engineering, Wonkwang University, Iksan, South Korea. His research interests include magnetic sensors and actuators, multiscale magnetic micro/nano systems, magnetic hyperthermia, and implantable medical devices.